On the Glass Transition Behavior, Interaction Energies, and Hydrogen-Bonding Strengths of Binary Poly(*p*-vinylphenol)/Polyether Blends

P. Pedrosa, J. A. Pomposo, E. Calahorra, and M. Cortazar*

Departamento de Ciencia y Tecnología de Polímeros, Facultad de Ciencias Químicas de San Sebastián, P.O. Box 1072, 20080 San Sebastián, Spain

Received May 13, 1993; Revised Manuscript Received October 4, 1993®

ABSTRACT: The miscibility behavior and the specific interactions of binary blends of poly(ethylene oxide) (PEO) and poly(vinyl methyl ether) (PVME) with poly(*p*-vinylphenol) (PVPh) are investigated by means of differential scanning calorimetry, analogue calorimetry, and Fourier transform infrared (FTIR) spectroscopy. The compositional variation of the glass transition temperature (T_g) of PEO/PVPh and PVME/PVPh blends is analyzed in terms of the Kovacs free volume theory. This theoretical approach is able to reproduce the glass transition behavior of both systems quite well, although excess volume measurements of PVME/PVPh blends do not support the physical meaning assigned to the parameters in the theory. The presence of specific interactions between the PVPh and the polyethers is indicated by the large and exothermic interaction energy density obtained both from heat of mixing data using model compounds and from melting point depression data of PEO/PVPh blends. The specific nature and the average strength of the intermolecular interaction for the polymer blends and the analogue mixtures are determined by means of FTIR measurements.

Introduction

Many miscible polymer systems show monotonic T_g–composition curves[1-3] that can be accounted for by several theoretical equations proposed in the literature.[4-8] The important role of specific interactions and their strength in determining the glass transition behavior of polymer blends is well recognized, and several predictive equations have been recently derived that incorporate these effects.[9,10]

However, a variety of miscible polymer–diluent mixtures and polymer blends show an unusual, but similar, compositional variation of the T_g, with two different well-defined curves that meet at a characteristic temperature. For polymer blends, the presence of this break, or cusp, in the T_g–composition curve was first noticed by Roy and co-workers[11] for the poly(methyl acrylate)/poly(vinyl acetate) system, as well as for three other systems previously reported in the literature. In this sense, Prud'homme and co-workers[12-14] have demonstrated that binary polystyrene/poly(vinyl methyl ether) (PVME), poly(ϵ-caprolactone)/nitrocellulose, and polyester/chlorinated polymer blends also exhibit this behavior. In addition, Nishio et al.[15] reported the presence of a cusp in the T_g–composition curve of the poly(vinyl alcohol)/poly(vinylpyrrolidone) system. In practice, the cusp appears only when the difference between the T_g values of the two components is higher than about 70 K. A theoretical framework to rationalize the above results is provided by the free volume theory proposed by Kovacs[16,17] for polymer/plasticizer systems. In particular, the modified version that includes an interaction parameter, g, to account for the excess volume upon mixing has been very useful in reproducing the experimental trends, despite the shortcomings and limitations of the theoretical approach. Moreover, information about interaction strengths from the Kovacs g parameter in qualitative agreement with that obtained from the classical Flory–Huggins χ parameter has been obtained for certain systems.[14] In this paper, the glass transition behavior of binary poly(*p*-vinylphenol) (PVPh)/PVME and PVPh/poly(ethylene oxide) (PEO) blends is reported, and Kovacs' free volume theory is employed to analyze the T_g–composition variation.

On the other hand, specific interactions between components such as hydrogen bonding,[18] dipole–dipole interactions,[19] acid–base interactions,[20] or transition-metal complexation[21] are frequently responsible for blend miscibility and determine to a large extent the magnitude of thermodynamic properties such as the volume of mixing or the enthalpy of mixing. A considerable effort has been made in recent years in order to identify the nature and strength of intermolecular interactions in polymer blends. In this sense, Fourier transform infrared (FTIR) spectroscopy has become very useful, because the technique is particularly sensitive to specific forces between polymer segments, especially hydrogen bonds. Thus, the presence of strong intermolecular hydrogen-bonding interactions between PVPh and ether-containing polymers has been clearly identified in the FTIR spectra of these blends.[22,23] Also, analogue calorimetry has provided valuable estimates of the interaction energy between polymers by recognizing that enthalpic interactions between functional groups are very similar for both polymer blends and model compound mixtures.[24-26] Both techniques are used in this work, as well as the melting point depression method, in order to achieve an indication of the intensity and the extent of the intermolecular interactions involved in PVPh/polyether blends. In addition, the influence of these specific forces on the excess volume of mixing is investigated for PVPh/PVME blends, and the experimental results are compared to the predictions from Kovacs' theory.

Summary of the Kovacs Free Volume Theory. The starting point is the assumption of the free volume additivity:[16]

$$f = \phi_1 f_1 + \phi_2 f_2 \tag{1}$$

where f is the free volume of the blend, f_i is the free volume of component i, and ϕ_i is its volume fraction. However, if the excess volume upon mixing is not negligible, eq 1 should be modified, as shown by Braun and Kovacs,[17] to

* To whom correspondence should be addressed.

® Abstract published in *Advance ACS Abstracts*, December 1, 1993.

0024-9297/94/2227-0102$04.50/0

take into account this effect:

$$f = \phi_1 f_1 + \phi_2 f_2 - V_e/V \quad (2)$$

where V is the volume of the blend and V_e is the excess volume. The last term in eq 2 is usually related to an interaction term (g) by means of

$$V_e/V = g\phi_1\phi_2 \quad (3)$$

where V_e is defined according to Braun and Kovacs[17] as

$$V_e = V_1 + V_2 - V \quad (4)$$

Hence, a positive g parameter results in a decrease of the free volume. In practice, an increase in the density of the blend is expected when strong specific interactions between its components are present.[27,28]

In the framework of the free volume theory, the temperature dependence of f_i is assumed to be linear as a first approximation, so

$$f_1 = f_{g1} + \Delta\alpha_1(T - T_{g1}) \quad (5)$$

$$f_2 = f_{g2} + \Delta\alpha_2(T - T_{g2}) \quad (6)$$

where f_{gi} is the fractional free volume of the component i at T_{gi} and $\Delta\alpha_i$ is the difference between the volume expansion coefficients in the liquid and glassy states. At the glass transition temperature of the blend, the fractional free volume is given by

$$f_g = \phi_1 f_{g1} + \phi_2 f_{g2} \quad (7)$$

The expression describing the composition dependence of T_g derived from the equations above is

$$T_g = \frac{\phi_2 T_{g2} + k\phi_1 T_{g1} + (g/\Delta\alpha_2)\phi_1\phi_2}{\phi_2 + k\phi_1} \quad (8)$$

where $k = \Delta\alpha_1/\Delta\alpha_2$ and the polymer in the blend with the higher T_g value is denoted as component 1. However, eq 8 is only valid for temperatures above a certain critical temperature (T_{crit}) given by:[16,17]

$$T_{crit} = T_{g1} - f_{g1}/\Delta\alpha_1 \quad (9)$$

At T_{crit}, the free volume of polymer 1 becomes zero, as well as below this temperature, since negative values of the free volume have no physical meaning. In this case, the composition dependence of T_g is given by:

$$T_g = T_{g2} + \frac{\phi_1 f_{g1} + g\phi_1\phi_2}{\phi_2\Delta\alpha_2} \quad (10)$$

In order to analyze the experimental data in terms of eq 10, it can be rearranged to

$$\frac{T_g - T_{g2}}{\phi_1} = \frac{g}{\Delta\alpha_2} + \left(\frac{f_{g1}}{\Delta\alpha_2}\right)\frac{1}{\phi_2} \quad (11)$$

so that, for $T < T_{crit}$, a plot of $(T_g - T_{g2})/\phi_1$ versus $1/\phi_2$ should give a straight line with slope $f_{g1}/\Delta\alpha_2$ and intercept $g/\Delta\alpha_2$. $\Delta\alpha_2$ and g can be calculated using the classical value of 0.025 for f_{g1}.[29,30] On the other hand, for $T > T_{crit}$, we can determine the k value using the value of $g/\Delta\alpha_2$ from $T < T_{crit}$, the experimental T_g data, and the following expression, derived from eq 8.

$$k = \frac{\phi_2(T_{g2} - T_g) + (g/\Delta\alpha_2)\phi_1\phi_2}{\phi_1(T_g - T_{g1})} \quad (12)$$

Slightly different values are usually obtained due to experimental uncertainties and, consequently, an average value of k is more representative. Finally, given $\Delta\alpha_2$ and k, it is also possible to estimate $\Delta\alpha_1$ from

$$\Delta\alpha_1 = k\Delta\alpha_2 \quad (13)$$

Table I. Polymers Used in This Work

polymer	wt-av mol wt	T_g (K)	source
PEO	300 000[a]	218	Polysciences, Inc.
PVME	56 400[b]	250	Aldrich Chemical Co.
PVPh	30 000[a]	428	Polysciences, Inc.

[a] Provided by supplier. [b] Measured by GPC.

Experimental Section

The characteristics of the polymers used in this work are given in Table I. Blends were prepared by mixing appropriate amounts of the components in 2% (w/v) tetrahydrofuran (THF) solutions. Films were obtained by evaporating the solvent at 323 K. Further solvent was then removed in a vacuum oven at 333 K for 2 weeks. This temperature was not found high enough to completely remove the solvent from blends with a high PVPh content. Consequently, an additional 3 h of drying at 423 K (under vacuum) was used to completely remove THF from the blends.

Thermal properties such as glass transition temperature (T_g) and melting temperature (T_m) were analyzed by differential scanning calorimetry (DSC) with a Perkin-Elmer DSC 2C apparatus equipped with a TADS microcomputer and calibrated with indium. In a first scan, the samples were heated from 150 to 423 K at 40 K/min and maintained at that temperature for 3 min to ensure well-defined and reproducible T_g's. The thermal transitions were recorded at a heating rate of 20 K/min in a second scan. Results from duplicate or triplicate samples and subsequent scans indicate an accuracy in the T_g data of ±1.5 K. T_g's were measured at the half-height of the corresponding heat capacity change, and the heat of fusion (ΔH_f) was calculated from the area of the corresponding peak. In all cases, the width of the glass transition region was expressed as the temperature interval between the onset and completion of the heat capacity change at T_g. The isothermal crystallization from the melt was also examined by DSC. The crystalline samples were melted at 373 K for 10 min to destroy all prior crystals, cooled quickly to the crystallization temperature (T_c), and then maintained at T_c until the crystallization proceeds to 10% of the overall process. Subsequently, the samples were heated at 10 K/min in order to determine the melting temperatures.

Specific volumes were determined at 298.2 K using a pycnometer calibrated with n-heptane (Aldrich; HPLC grade). The temperature of the water bath was kept constant to within 0.1 K, and the measured values were found to be accurate to ±0.001 cm^3/g from repeated measurements.

Heats of mixing for low molecular weight analogues of the corresponding polymers were measured using a Setaram C80D flux-type calorimeter. 4-Ethylphenol (EPH) was selected as the analogue of PVPh and 2,4-dimethoxypentane (DMOP) was employed as the model compound of PVME. Diethylene glycol diethyl ether (DEGDEE), diethylene glycol dimethyl ether (DEGDME), and ethylene glycol diethyl ether (EGDEE) were assumed to closely resemble the PEO chemical structure and therefore used as model compounds of this polymer. Table II shows the molecular structures, densities, and molecular weights of the analogues used. EPH, DEGDEE, DEGDME, and EGDEE were obtained from Aldrich (≥98% pure). They were used as received without further purification. DMOP was synthesized by methylation of racemic 2,4-pentanediol (Aldrich; 99% pure) following a method similar to the Williamson synthesis.[31-33] The product was purified by distillation and characterized by ^{13}C and ^{1}H NMR. The heats of mixing were measured at 338.2 ± 0.1 K, a temperature above the melting point of EPH and below the boiling point of all the model compounds employed in this work.

Infrared spectra were recorded with a Nicolet 5 DXC spectrometer. Thin films of the blends were cast from 1% (w/v) THF solutions onto potassium bromide windows at room temperature. The drying conditions were identical to those used for DSC measurements. A minimum of 64 scans were signal averaged at a resolution of 2 cm^{-1}. The hydroxyl stretching region of the IR spectrum was analyzed, both for the blends and for the

Table II. Model Compounds for the Polymers Investigated

compd	structure	density[a] (g/cm³)	mol wt
EPH	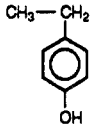	0.976	122.2
DMOP	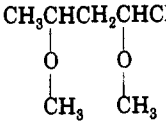	0.728	132.0
DEGDEE	$CH_3CH_2OCH_2CH_2OCH_2CH_2OCH_2CH_3$	0.865	162.0
DEGDME	$CH_3OCH_2CH_2OCH_2CH_2OCH_3$	0.897	134.2
EGDEE	$CH_3CH_2OCH_2CH_2OCH_2CH_3$	0.795	118.2

[a] At 338.2 K.

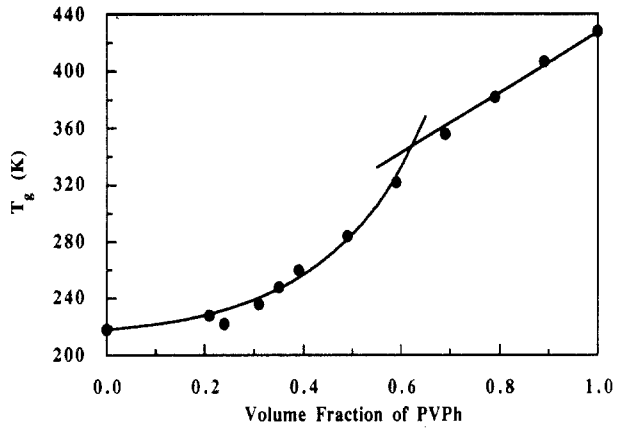

Figure 1. Composition dependence of the glass transition temperature for the PEO/PVPh blend. The continuous lines are the prediction from Kovacs' theory (eqs 8 and 10) using parameters from Table IV. Error bars are approximately of the same size as the points represented.

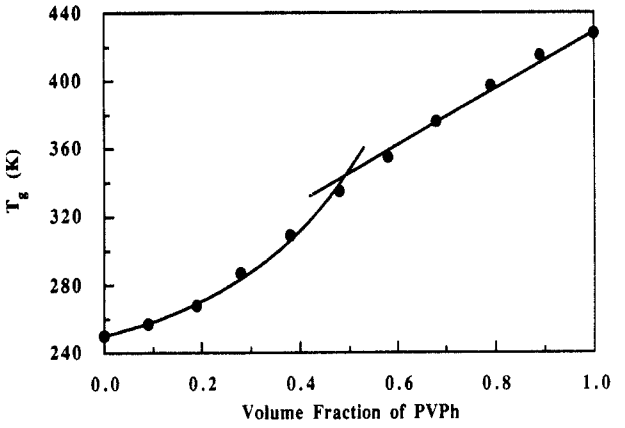

Figure 2. Composition dependence of the glass transition temperature for the PVME/PVPh blend. The continuous lines are the prediction from Kovacs' theory (eqs 8 and 10) using parameters from Table IV. Error bars are approximately of the same size as the points represented.

model compound mixtures. Spectra at elevated temperatures were obtained by using a SPECAC high-temperature cell, mounted in the spectrometer, with an accuracy of ±2 °C.

Results and Discussion

A. Glass Transition Behavior. The miscibility of PEO/PVPh and PVME/PVPh blends has been ascertained by the determination of a single, composition-dependent, glass transition temperature. Figures 1 and 2 show the T_g–composition curves of both systems as a function of the volume fraction of PVPh. For the PEO/PVPh system, a correction has been made in order to take into account the true composition of the amorphous phase when crystallization takes place. Table III shows the degree of crystallinity measured for these compositions as well as the real composition of the amorphous phase.

Table III. Crystallinity Degree and Amorphous Composition of Crystalline PEO/PVPh Blends (ϕ_{PVPh})

wt % PVPh	% crystallinity[a]	ϕ_{PVPh}	T_g (K)
0	68.4	0.00	218
10	57.5	0.21	228
20	19.6	0.24	222
30	4.9	0.31	236
35	1.8	0.35	248

[a] Calculated as the ratio of the experimental heat of fusion to that of 100% crystalline PEO.[34]

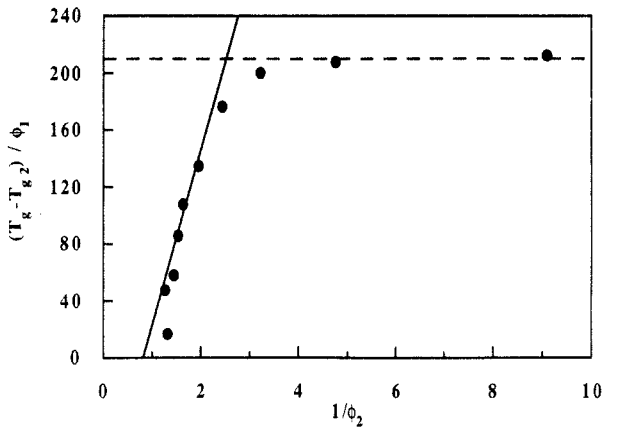

Figure 3. Analysis of the experimental data for PEO/PVPh blends according to Kovacs' theory (—). The additivity rule is represented by the dashed line.

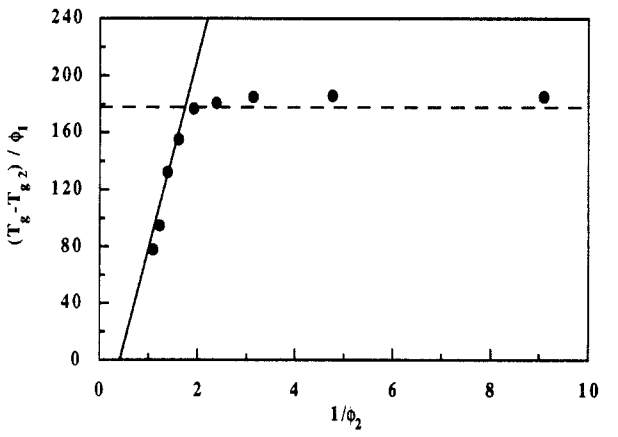

Figure 4. Analysis of the experimental data for PVME/PVPh blends according to Kovacs' theory (—). The additivity rule is represented by the dashed line.

According to the single-T_g criterion, both systems are miscible across the full composition range, although the experimental T_g–composition curves do not follow a simple monotonic function but appear to contain two well-defined regions separated by a singular point or cusp. This behavior has been shown to occur, in the framework of the free volume theory,[16,17] when the difference between the T_g's of the components is large enough to allow the free volume of the high-T_g polymer to vanish at a critical temperature T_{crit}. An improved analysis of the experimental data for $T < T_{crit}$ can be made in terms of this theory using eq 11 as shown in Figures 3 and 4. T_g data below T_{crit} can be fitted to a straight line from which the parameters g and $\Delta\alpha_2$ can be determined using the classical value of 0.025 for f_{g1}.[29,30] On the other hand, the glass transition behavior above T_{crit} is given by eq 8. However,

Table IV. Parameters of Kovacs' Free Volume Theory for PEO/PVPh and PVME/PVPh Blends

system	$\Delta\alpha_1$ (K^{-1})	$\Delta\alpha_2$ (K^{-1})	k	g	T_{crit} (K)	ϕ_1^{crit}
PEO/PVPh	3.11×10^{-4}	2.22×10^{-4}	1.40 ± 0.17	−0.020	348	0.62
PVME/PVPh	2.97×10^{-4}	2.02×10^{-4}	1.47 ± 0.14	−0.011	344	0.49

Table V. Specific Volumes of PVME/PVPh Blends at 298.2 K

wt % PVPh	V_{sp} (cm^3/g)	wt % PVPh	V_{sp} (cm^3/g)
0	0.957	75	0.862
25	0.919	100	0.849
50	0.892		

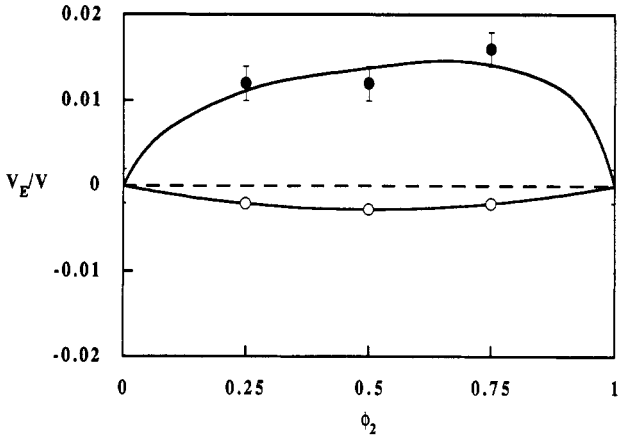

Figure 5. Excess volume of mixing (see eq 4) for the PVME/PVPh blend at 298.2 K: (●) experimental; (○) predicted by Kovacs' theory with the g parameter taken from Table IV.

due to the lack of the experimental $\Delta\alpha_1$ values, we have used the T_g results above T_{crit} to calculate $\Delta\alpha_1$ by means of eqs 12 and 13. Table IV summarizes the parameters determined for PEO/PVPh and PVME/PVPh blends as well as the cusp temperatures (T_{crit}) and the related critical compositions ϕ_1^{crit}.

The thermal expansion coefficients of PEO, PVME, and PVPh reported in Table IV are in the usual range found for most vinyl polymers, e.g., $1.5 < \Delta\alpha < 6$ (10^{-4} K^{-1}).[35] Also, good agreement has been found for the value of the coefficient of thermal expansion of PVPh, $\Delta\alpha_1$, estimated from both the PEO/PVPh and PVME/PVPh systems. Hence, the critical temperature predicted by the theory for PVPh (eq 9) is almost the same in both cases, e.g., 346 ± 2 K. The corresponding ϕ_1^{crit} for each system is however slightly different since it is highly sensitive to the actual ($T_{g1} - T_{g2}$) value.

Negative values of the Kovacs g parameter have been obtained for both systems and, consequently, an increase of the free volume (eq 2) is expected from the T_g analysis of these systems. The experimental specific volumes of PVME/PVPh blends are summarized in Table V, and a comparison of the experimental and predicted excess volumes of mixing (defined according to eq 4) are shown in Figure 5. A striking feature in this case is the disagreement between theoretical predictions and experimental results. However, a similar density increase upon mixing poly(oxymethylene) and PVPh has also been observed by Machado and French.[36] Although the excess volume is the result of several different and often competing factors,[37,38] the above results can be rationalized in terms of strong hydrogen-bonding interactions between PVPh and polyethers promoting shorter intermolecular distances at the expense of the free volume. Hence, it could be more appropriate, at least for these systems, to take the g parameter as a merely adjustable parameter

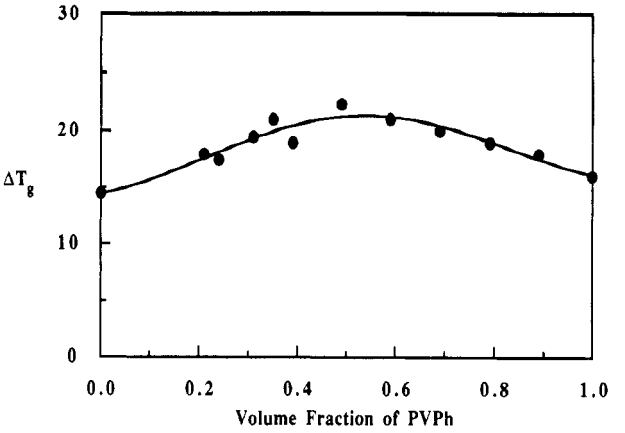

Figure 6. Composition dependence of the glass transition widths for the PEO/PVPh system. The continuous line is intended only as a visual guide.

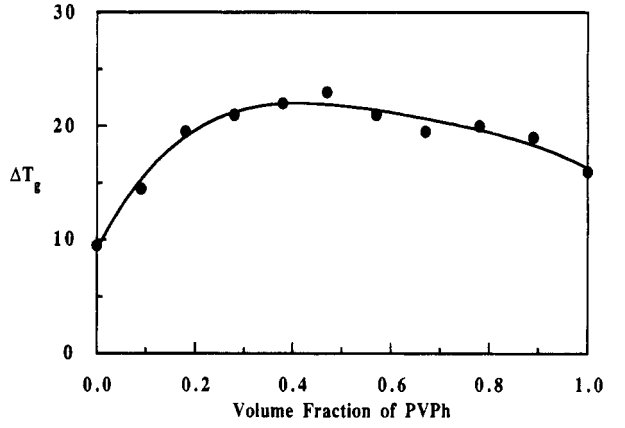

Figure 7. Composition dependence of the glass transition widths for the PVME/PVPh system. The continuous line is intended only as a visual guide.

rather than identify it with an interactional term. In the absence of experimental data, the same statement is also valid for the $\Delta\alpha_i$ parameters.

Despite the shortcomings of the theory (e.g., an iso-free-volume transition is assumed and the dependences of the free volume on molecular weight, chain stiffness and geometry, intermolecular forces, etc., are not taken into account), it predicts the presence of a cusp in the T_g–composition curve of miscible blends involving PVPh at a T_{crit} given by eq 9. Interestingly, the T_g results of Belfiore and co-workers[39] concerning PVPh/linear polyester blends as well as those of Landry et al.[40] for PVPh/etheric polyphosphazenes are consistent with this theoretical prediction.

In order to obtain additional information about the blend homogeneity of PVPh/polyether blends, we have also measured the corresponding glass transition widths (see Figures 6 and 7). As seen for many systems,[41-43] the glass transition width for midrange compositions is larger than those of the pure components. This departure from width additivity is usually attributed to frozen-in local concentration fluctuations related to the level of interaction between blend components, since a broadening of the glass transition zone has been found experimentally for many systems when the blend interactions weaken.[41] In our case, the PVME/PVPh system shows a slightly larger deviation from additivity than the PEO/PVPh system. Following the transition width criterion above, a slightly more favorable interaction energy might be involved for PEO/PVPh blends than for PVME/PVPh blends. A similar conclusion is obtained from heat of mixing mea-

Table VI. Equilibrium Melting Temperatures of Pure PEO and Crystalline PEO/PVPh Compositions As Determined by DSC

wt % PEO	$T_m°$ (K)	wt % PEO	$T_m°$ (K)
100	342	70	338
90	340	65	336
80	339		

surings using model compounds, as will be demonstrated below.

B. Interaction Energies. The melting point depression technique is a valuable method for measuring the interaction energy density between PEO and PVPh. The equilibrium melting temperatures of pure PEO and the crystalline blend compositions are listed in Table VI. They were determined by DSC[44] employing the Hoffman–Weeks method.[45]

The melting point depression ($\Delta T_m°$) of a semicrystalline polymer caused by the addition of a miscible polymeric diluent is related to the interaction energy density (B_{12}) by:[46]

$$\Delta T_m° = -B_{12}(V_{2u}/\Delta H_{2u})T_m°\phi_1^2 \qquad (14)$$

A value of $B_{12} = -7.1$ cal/cm^3 was obtained from a linear regression of the data in Table IV using the following literature values:[34] $V_{2u} = 38.9$ cm^3/mol and $\Delta H_{2u} = 2.1$ kcal/mol. The B_{12} value is close to that reported previously by Belfiore and co-workers[23] (−10.2 cal/cm^3), taking into account that a low-molecular-weight PVPh and nonequilibrium melting temperatures were used by these authors. Once again, the presence of specific interactions between components is pointed out in the large negative value of B_{12}.

It should be noted that the B_{12} parameter obtained from the melting point depression technique generally contains both enthalpic (B_{12}^h) and excess entropic contributions (B_{12}^s).[26,47,48] Consequently, it can be expressed as[49]

$$B_{12} = B_{12}^h - TB_{12}^s \qquad (15)$$

An estimation of the enthalpic contributions, B_{12}^h, can be achieved by means of heat of mixing measurements employing low-molecular-weight model compounds by recognizing that enthalpic interactions are mainly determined by contacts between nearest-neighbor functional groups.[24-26] In this sense, we have selected appropriate model compounds of PEO/PVPh and PVME/PVPh blends (Table II) in order to measure the heats of mixing for analogue mixtures of the corresponding polymer blends. Figure 8a shows the heats of mixing for binary mixtures of EPH as the analogue of PVPh and several model compounds of PEO such as DEGDEE, DEGDME, and EGDEE. A good agreement between data derived using these model compounds is found in spite of their slightly different chemical structures. The corresponding enthalpic interaction energy density (B_{12}^h) is given by

$$B_{12}^h = (\Delta H_m/V)/\phi_1\phi_2 \qquad (16)$$

The dependence of B_{12}^h on the volume fraction of EPH (ϕ_{EPH}) for these mixtures is represented in Figure 8b. A linear relationship is experimentally found, that can be expressed as

$$B_{12}^h = -18.62 - 28.30\phi_{EPH} \quad (\text{cal/cm}^3) \qquad (17)$$

A comparison between the enthalpic B_{12}^h parameter given by eq 17 for the analogue mixtures and the interaction (free) energy parameter (B_{12}) of PEO/PVPh blends reveals substantial differences between them. First, B_{12}^h from eq 17 has a strong composition dependence, whereas B_{12} from melting point depression appears to be constant in the range of PEO weight fractions between 0.65 and 0.9. Second, the value of B_{12}^h in the range of compositions are considerably higher than the value of B_{12} for PEO/PVPh blends. In terms of eq 15, this can be explained as a consequence of two different factors: the enthalpic contribution to B_{12} for analogue mixtures is very different from that of PEO/PVPh blends, and/or excess entropic contributions play an important role in the PEO/PVPh system. In the latter case, an unfavorable (negative) excess entropy contribution should be involved since $|B_{12}| < |B_{12}^h|$. Physically, a loss of entropy upon mixing can be expected as a result of some kind of ordering in the blend due to the formation of directional-specific interactions.[50] Since hydrogen-bonding interactions play a key role in explaining the miscibility of PEO/PVPh blends,[22,23] the balance between the number and strength of hydrogen bonds broken (in pure PVPh) and formed upon mixing (in the blend) probably determines the magnitude and the sign of the presumed excess entropic contributions.

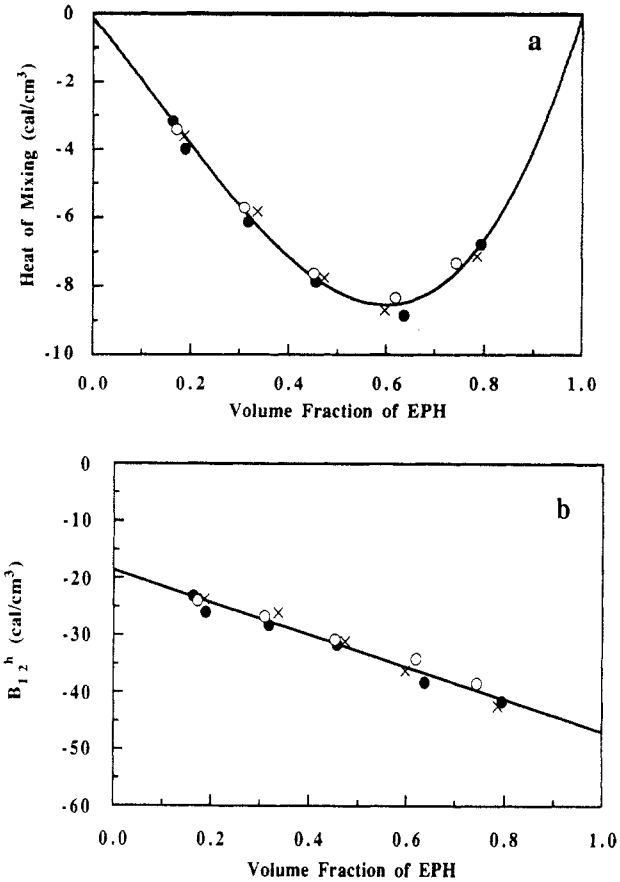

Figure 8. (a) Heats of mixing of EPH with DEGDEE (●), DEGDME (×), and EGDEE (○) at 338.2 K and (b) dependence of the enthalpic interaction energy density on the volume fraction of EPH for the same mixtures.

Information about B_{12} from melting point depression cannot be obtained for PVME/PVPh blends because in this case both components are amorphous. Heats of mixing data using EPH as the model compound of PVPh and DMOP as a close analogue of PVME are represented in Figure 9a. The corresponding B_{12}^h parameter is shown in Figure 9b as a function of composition. A linear relationship is also found for the compositions investigated:

$$B_{12}^h = -17.43 - 19.72\phi_{EPH} \quad (\text{cal/cm}^3) \qquad (18)$$

In this case, the values of B_{12}^h are slightly less exothermic than that corresponding to analogue mixtures of PEO/PVPh blends.

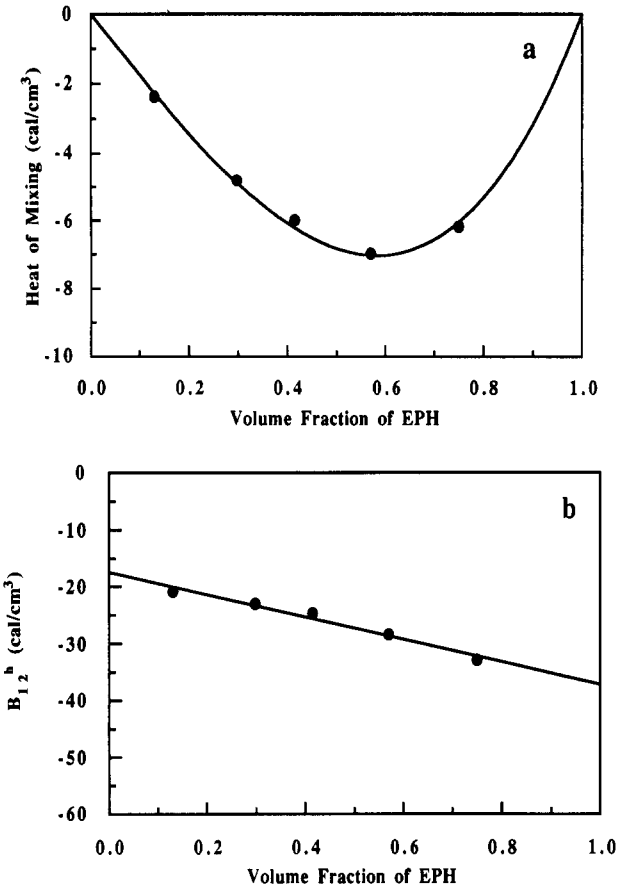

Figure 9. (a) Heats of mixing of EPH with DMOP at 338.2 K and (b) dependence of the enthalpic interaction energy density on the volume fraction of EPH for the same mixture.

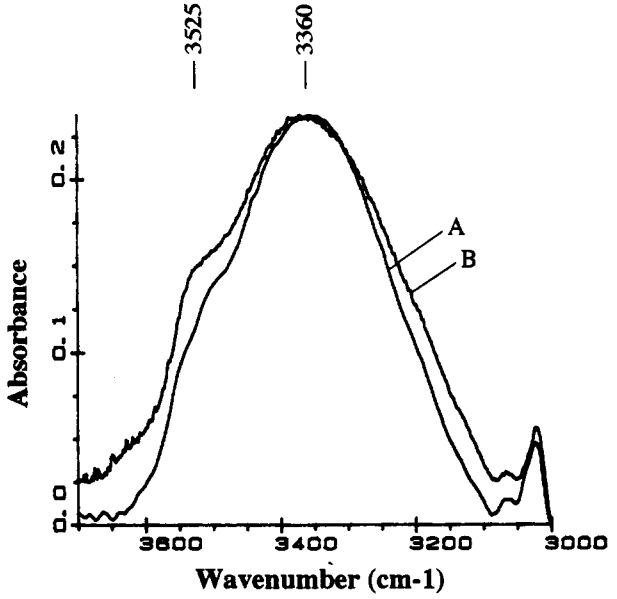

Figure 10. Hydroxyl stretching region of the FTIR spectra at 298 K for (A) EPH and (B) PVPh.

Interestingly, FTIR measurements enable one to estimate the average hydrogen-bonding interaction strengths for the mixtures of model compounds and for the polymer blends. In the following section the FTIR results are analyzed and compared to those from analogue calorimetry.

C. Hydrogen-Bonding Interaction Strengths. The hydroxyl stretching regions of the FTIR spectra of EPH and PVPh at 298 K are shown in Figure 10. It has been shown[22,23] that the narrow band appearing as a shoulder

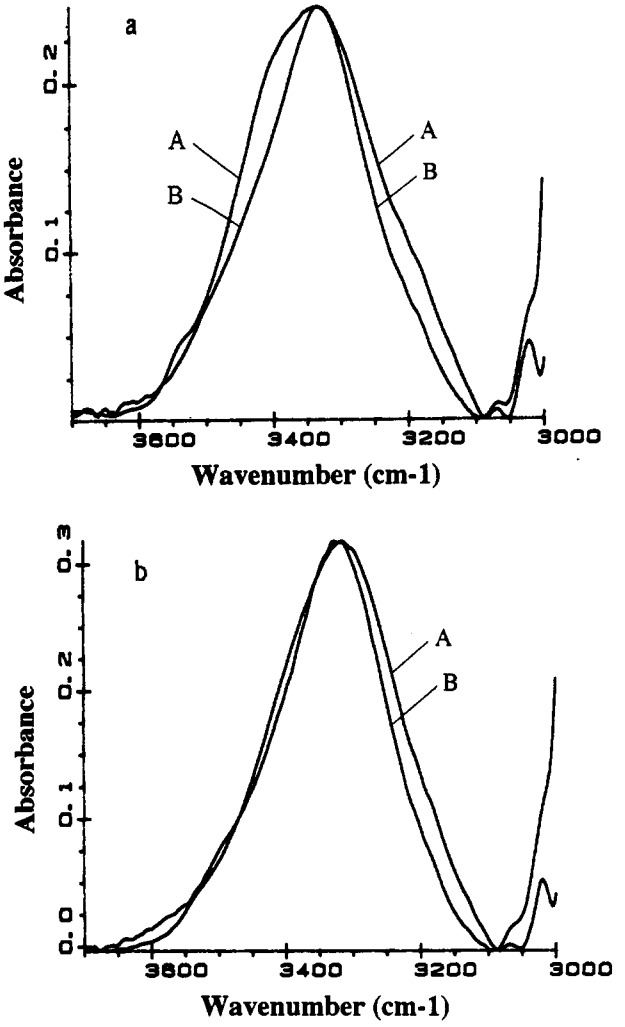

Figure 11. (a) Hydroxyl stretching region of the FTIR spectra for DMOP/EPH mixtures at 298 K: (A) 40/60 wt %; (B) 80/20 wt %. (b) Hydroxyl stretching region of the FTIR spectra for PVME/PVPh blends at 298 K: (A) 40/60 wt %; (B) 80/20 wt %.

at higher wavenumbers (ca. 3525 cm^{-1}) is due to free (unassociated) hydroxyl (OH) groups, while the broad band at lower wavenumbers (ca. 3350–3370 cm^{-1}) corresponds to a wide distribution of (self-associated) hydrogen-bonded OH groups. The frequency difference ($\Delta\nu$) between the free hydroxyl absorption and that of the hydrogen-bonding species provides a measure of the average strength of the hydrogen-bonding interaction.[51] For both EPH and PVPh, the value of $\Delta\nu$ is about 165 cm^{-1}.

Figure 11a shows spectra in the hydroxyl stretching region of DMOP/EPH mixtures at 298 K. As can be seen, the hydrogen-bonded hydroxyl band of EPH shifts to lower frequencies and narrows considerably in the presence of DMOP. In addition, the intensity of the band corresponding to free OH groups is observed to decrease significantly in DMOP/EPH mixtures. All these features are indicative of strong interactions between the hydroxyl groups of EPH and etheric oxygens of DMOP. The average strength of this intermolecular hydrogen-bonding interaction, as measured by $\Delta\nu$, is about 190 cm^{-1} (Table VII), whereas that corresponding to self-association of hydroxyl groups in pure EPH is considerably smaller ($\Delta\nu$ = 165 cm^{-1}). The FTIR spectra of PVME/PVPh blends in the region between 3700 and 3000 cm^{-1} at 298 K are illustrated in Figure 11b. The shape and position of the hydroxyl stretching band for the polymer blend are very similar to those of the analogue mixture. Hence, the average intensity of the hydrogen-bonding interaction is almost

Table VII. Frequency Difference $\Delta\nu$ (cm^{-1}) between the Free Hydroxyl Absorption and That of the Hydrogen-Bonded Groups for Polyether/PVPh Blends and Analogue Mixtures at 298 K

	composition (wt %)			composition (wt %)	
	40/60	80/20		40/60	80/20
DMOP/EPH	190	193	DEGDME/EPH	160	173
PVME/PVPh	209	203	POE/PVPh	185	270

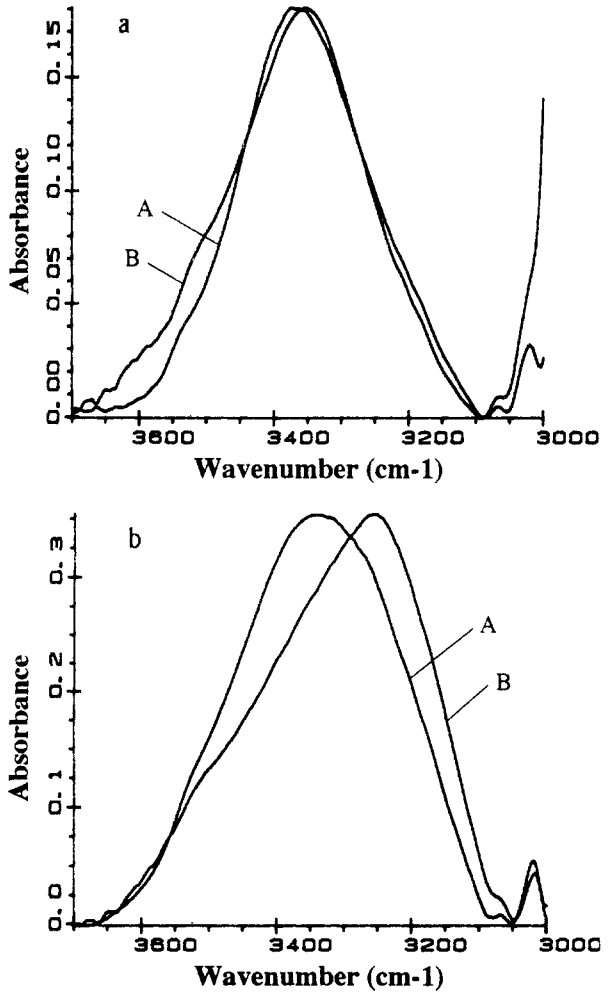

Figure 12. (a) Hydroxyl stretching region of the FTIR spectra for DEGDME/EPH mixtures at 298 K: (A) 40/60 wt %; (B) 80/20 wt %. (b) Hydroxyl stretching region of the FTIR spectra for PEO/PVPh blends at 298 K: (A) 40/60 wt %; (B) 80/20 wt %.

the same for PVME/PVPh and DMOP/EPH mixtures (Table VII), suggesting that the hydrogen-bonding environment is similar for the polymer blend and the mixture of model compounds.

The hydroxyl stretching region of the FTIR spectra of DEGDME/EPH mixtures at 298 K is shown in Figure 12a. In this case, the infrared frequency shifts are about 30 cm^{-1} less than those corresponding to DMOP/EPH mixtures, so it can reasonably be deduced that the mean specific interaction between EPH and DEGDME is weaker than the intermolecular EPH/DMOP interaction. Similar results were obtained when EGDEE or DEGDEE were employed instead of DEGDME. Although the strength of the hydrogen-bonding interactions appears to be slightly increased in the DMOP/EPH system, the number of such specific contacts may differ significantly for DMOP/EPH and DEGDME/EPH mixtures. Indeed, the heats of mixing of DEGDME/EPH mixtures are slightly more exothermic than those of DMOP/EPH mixtures. The

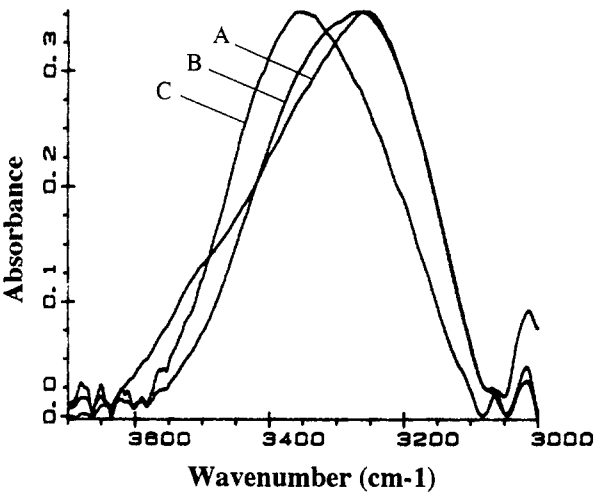

Figure 13. Hydroxyl stretching region of the FTIR spectra of a PEO/PVPh 80/20 wt % blend at several temperatures: (A) 298, (B) 375, and (C) 433 K.

increased steric hindrance of the methyl groups attached to the etheric oxygens of DMOP may be responsible for this behavior. The FTIR results of PEO/PVPh blends in the 3700–3000-cm^{-1} range at 298 K are illustrated in Figure 12b. The essential features of these spectra are in good agreement with data published previously for the same system.[22,23] The spectrum corresponding to the blend with 40 wt % PEO is broader than that shown in Figure 12a for the analogue mixture and shows a significant wavenumber shift to lower frequency (Table VII). The hydroxyl stretching band of the blend with 80 wt % PEO is even more asymmetric, and the maximum of the band shifts to about 3255 cm^{-1}. In order to ascertain if crystallization of PEO is responsible for this behavior, the FTIR spectrum of the blend with 80 wt % was recorded at 375 K (above the melting point of PEO). As shown in Figure 13, the location of the band remains unaltered upon melting the PEO crystalline phase, suggesting that the shape and position of the hydroxyl stretching band is indeed a strong function of blend composition. On the other hand, the OH region of the FTIR spectra of PEO/PVPh blends does not resemble that of DEGDME/EPH mixtures, until the temperature is sufficiently raised (Figure 13). From these results we can conclude that the hydrogen-bonding environment of PEO/PVPh blends differs considerably from that of the analogue mixtures. The same statement is valid when the hydroxyl stretching regions of the FTIR spectra of PEO/PVPh and PVME/PVPh blends are compared. In fact, Le Menestrel et al.[52] have also noticed that the PVPh/PEO specific interaction is considerably stronger than those of PVPh/poly(vinyl alkyl ethers), so they consider PEO and poly(oxymethylene) to be special cases. The results from this work also support this claim.

Conclusions

The miscibility behavior and the specific interactions between PVPh and two representative polyethers were investigated. Binary blends of PEO and PVME with PVPh were found to be miscible across the entire composition range, although the compositional variation of T_g in both systems shows an anomalous break or cusp. The experimental results were analyzed in terms of the Kovacs free volume theory.[16,17] In spite of the well-known shortcomings of this theoretical approach, it is able to reproduce the experimental behavior of PEO/PVPh blends quite well. In addition, the presence of a similar cusp in the T_g–composition curves of other very different systems involving PVPh, such as PVPh/linear polyester[39] and

PVPh/etheric polyphosphazenes,[40] is in agreement with the predictions from the theory.

The presence of specific interactions promoting miscibility between PEO and PVPh was pointed out in the large negative value of the interaction (free) energy density, B_{12}, derived from equilibrium melting point depression measurements. The heats of mixing of analogue mixtures of both PEO/PVPh and PVME/PVPh blends also indicate that strong interactions occur between model compounds, but the enthalpic interaction energy density was found to be significantly more exothermic for the low-molecular-weight models of the polymers. In this sense, a significant difference could be expected if excess entropic contributions arising from directionally specific interactions[50] and/or free volume, or equation of state, effects[53,54] are not negligible.

The specific nature of the interactions was determined by means of FTIR measurements on both the polymer blends and the analogue mixtures. Thus, the frequency shift to lower wavenumbers that appears in the hydroxyl stretching region of the corresponding FTIR spectra suggests the presence of hydrogen-bonding interactions involving OH groups attached to phenolic rings on the one hand and etheric oxygens on the other. These intermolecular interactions were stronger than phenolic self-association, as revealed by the frequency shift observed. The average strength of the specific interactions was almost the same for PVME/PVPh blends and DMOP/EPH mixtures, pointing to a similar hydrogen-bonding environment in both systems. Conversely, significant differences in both the frequency shift and the shape of the OH band were found when the FTIR spectra of PEO/PVPh blends and DEGDME/EPH mixtures were compared. It has been shown that the crystallization of PEO is not responsible of this behavior. The FTIR results suggest an increased level of interaction between PEO and PVPh compared to that between PVME and PVPh, in agreement with DSC results concerning glass transition widths.

The presence of specific interactions between components was also pointed out in the density increase observed upon mixing for PVME/PVPh blends. The experimental excess volumes of mixing were found far apart from those predicted by the Kovacs free volume approach; hence, the physical meaning attributed to the parameters in this theory has been questioned. Nevertheless, in the absence of a better theory, the Kovacs approach can be employed to obtain, at least, a semiquantitative location of the cusp that appears in the experimental T_g–composition curve of many miscible polymer blends.

Acknowledgment. Financial support of this work by UPV/EHU (Project No. 203215-EB096/92) is gratefully acknowledged. We also thank L. A. Belfiore for providing us with the completed version of the PVPh/polyester phase diagrams before publication.

References and Notes

(1) Utracki, L. A. *Polymer Alloys and Blends*; Hansen: New York, 1989.
(2) Solc, K. *Polymer Compatibility and Incompatibility*; MMI Press: New York, 1982.
(3) Roe, R. J. *Encyclopedia of Polymer Science and Engineering*, 2nd ed.; Mark, H. F., Bikales, N. M., Overberger, C. G., Menges, G., Eds.; John Wiley: New York, 1988; Vol. 7, p 531.
(4) Gordon, M.; Taylor, J. S. *J. Appl. Chem.* **1952**, *2*, 493.
(5) Fox, T. G. *Bull. Am. Phys. Soc.* **1956**, *1*, 123.
(6) Couchman, P. R. *Macromolecules* **1978**, *11*, 1156.
(7) Kwei, T. K. *J. Polym. Sci., Polym. Lett. Ed.* **1984**, *22*, 307.
(8) Brekner, M. J.; Schneider, H. A.; Cantow, H. J. *Polymer* **1988**, *29*, 78.
(9) Painter, P. C.; Graf, J. F.; Coleman, M. M. *Macromolecules* **1991**, *24*, 5630.
(10) Xinya, L.; Weiss, R. A. *Macromolecules* **1992**, *25*, 3242.
(11) Nandi, A. K.; Mandal, B. M.; Bhattacharya, S. N.; Roy, S. K. *Polymer Commun.* **1986**, *27*, 151.
(12) Aubin, M.; Prud'homme, R. E. *Polym. Eng. Sci.* **1988**, *28*, 1355.
(13) Jutier, J. J.; Lemieux, E.; Prud'homme, R. E. *J. Polym. Sci., Polym. Phys. Ed.* **1988**, *26*, 1313.
(14) Aubin, M.; Prud'homme, R. E. *Macromolecules* **1988**, *21*, 2945.
(15) Nishio, Y.; Haratani, T.; Takahashi, T. *J. Polym. Sci., Polym. Phys. Ed.* **1990**, *28*, 355.
(16) Kovacs, A. J. *Adv. Polym. Sci.* **1963**, *3*, 394.
(17) Braun, G.; Kovacs, A. J. *Physics of Non-Crystalline Solids*; Prins, J. A., Ed.; North-Holland: Amsterdam, The Netherlands, 1965; p 303.
(18) Coleman, M. M.; Graf, J. F.; Painter, P. C. *Specific Interactions and the Miscibility of Polymer Blends*; Technomic Publishing Co.: Lancaster, PA, 1991.
(19) Woo, E. M.; Barlow, J. W.; Paul, D. R. *J. Appl. Polym. Sci.* **1983**, *28*, 1347.
(20) Fowkes, F. M.; Tischler, D. O.; Wolfe, J. A.; Lannigan, L. A.; Ademu-John, C. M.; Halliwell, M. J. *J. Polym. Sci., Polym. Chem. Ed.* **1984**, *22*, 547.
(21) Sen, A.; Weiss, R. A. *Polym. Mater. Sci. Eng.* **1988**, *58*, 981.
(22) Moskala, E. J.; Varnell, D. F.; Coleman, M. M. *Polymer* **1985**, *26*, 228.
(23) Qin, C.; Pires, A. T. N.; Belfiore, L. A. *Polymer* **1990**, *31*, 177.
(24) Walsh, D. J.; Cheng, G. L. *Polymer* **1984**, *25*, 499.
(25) Rodgers, P. A.; Paul, D. R.; Barlow, J. W. *Macromolecules* **1991**, *24*, 4101.
(26) Landry, C. J. T.; Teegarden, D. M. *Macromolecules* **1991**, *24*, 4310.
(27) Fried, J. R.; Karasz, F. E.; Macknight, W. J. *Macromolecules* **1978**, *11*, 150.
(28) Chiou, J. S.; Paul, D. R. *J. Appl. Polym. Sci.* **1987**, *34*, 1503.
(29) Williams, M. L.; Landel, R. F.; Ferry, J. D. *J. Am. Chem. Soc.* **1955**, *77*, 3701.
(30) Ferry, J. D. *Viscoelastic Properties of Polymers*; John Wiley: New York, 1961.
(31) Williamson, A. W. *J. Chem. Soc.* **1952**, *4*, 229.
(32) Matsuzaki, K.; Sakota, K.; Okada, M. *J. Polym. Sci., Polym. Phys. Ed.* **1969**, *7*, 1444.
(33) Jursic, B. *Tetrahedron* **1988**, *44*, 6677.
(34) Van Krevelen, D. W. *Properties of Polymers*; Elsevier Scientific Publishing Co.: Amsterdam, The Netherlands, 1976.
(35) Brandrup, J.; Immergut, E. H., Eds. *Polymer Handbook*, 2nd ed.; Wiley-Interscience: New York, 1975.
(36) Machado, J. M.; French, R. N. *Polymer* **1992**, *33*, 760.
(37) Huu Tra Van; Patterson, D. *J. Solution Chem.* **1982**, *11*, 793.
(38) Costas, M.; Patterson, D. *J. Solution Chem.* **1982**, *11*, 807.
(39) Belfiore, L. A.; Qin, C.; Ueda, E.; Pires, A. T. N. *J. Polym. Sci., Polym. Phys. Ed.* **1993**, *31*, 409.
(40) Landry, C. J. T.; Ferrar, W. T.; Teegarden, D. M.; Coltrain, B. K. *Macromolecules* **1993**, *26*, 35.
(41) Fernandes, A. C.; Barlow, J. W.; Paul, D. R. *J. Appl. Polym. Sci.* **1986**, *32*, 5481.
(42) Schneider, H. A.; Cantow, H. J.; Wendland, C.; Leikauf, B. *Makromol. Chem.* **1990**, *191*, 2377.
(43) Pomposo, J. A.; Eguiazabal, I.; Calahorra, E.; Cortazar, M. *Polymer* **1993**, *34*, 95.
(44) Pedrosa, P.; Pomposo, J. A.; Calahorra, E.; Cortazar, M. *Polymer*. Submitted for publication.
(45) Hoffman, J. D.; Weeks, J. L. *J. Res. Natl. Bur. Stand.* **1962**, *66*, 13.
(46) Nishi, T.; Wang, T. T. *Macromolecules* **1975**, *8*, 909.
(47) Jo, W. H.; Kwon, I. H. *Macromolecules* **1991**, *24*, 3368.
(48) Kwon, I. H.; Jo, W. H. *Makromol. Chem., Theory Simul.* **1993**, *2*, 37.
(49) Barnum, R. S.; Goh, S. H.; Barlow, J. W.; Paul, D. R. *J. Polym. Sci., Polym. Lett. Ed.* **1985**, *23*, 395.
(50) ten Brinke, G.; Karasz, F. E. *Macromolecules* **1984**, *17*, 815.
(51) Purcell, K. F.; Drago, R. S. *J. Am. Chem. Soc.* **1967**, *89*, 2874.
(52) Le Menestrel, C.; Bhagwager, D. E.; Painter, P. C.; Coleman, M. M. *Macromolecules* **1992**, *25*, 7101.
(53) Patterson, D.; Robard, A. *Macromolecules* **1978**, *11*, 690.
(54) Sanchez, I. C.; Lacombe, R. H. *Macromolecules* **1978**, *11*, 1145.